International Journal of Innovative
Computing, Information and Control
Volume **12**, Number **4**, August **2016**

 ISSN 1349-4198
pp. 1073–1087

USE OF A RIEMANNIAN MANIFOLD TO IMPROVE THE THROUGHPUT OF A PRODUCTION FLOW SYSTEM

Kenji Shirai[1] and Yoshinori Amano[2]

[1]Faculty of Information Culture
Niigata University of International and Information Studies
3-1-1, Mizukino, Nishi-ku, Niigata 950-2292, Japan
shirai@nuis.ac.jp

[2]Kyohnan Elecs Co., LTD.
8-48-2, Fukakusanishiura-cho, Fushimi-ku, Kyoto 612-0029, Japan
y_amano@kyohnan-elecs.co.jp

Received January 2016; revised May 2016

Abstract. *Bottlenecks in production processes often result from worker volatility or delivery delays caused by other companies. The theory of constraints states that synchronizing the bottlenecks may improve the throughput of the process. However, the standard in physical restraint is not quantitatively shown in the production system. In this study, we propose the quantitative use of a Riemannian manifold to improve the throughput of a production flow system. We present a stochastic throughput model for producing the propagation necessary to measure synchronization. We also introduce a Fisher information matrix to specify volatility. We verify this method via a dynamic simulation of a production flow system. Finally, we present the synchronous and asynchronous data obtained using the production flow system.*

Keywords: Riemannian manifold, Fisher information matrix, Diffusion process, Langevin equation, Production process

1. **Introduction.** Based on mathematical and physical understandings of production engineering, we are conducting research aimed at establishing an academic area called mathematical production engineering. As our business size is a small-to-medium-sized enterprise, human intervention constitutes a significant part of the production process, and revenue can sometimes be greatly affected by human behavior. Therefore, when considering human intervention from outside companies, a deep analysis of the production process and human collaboration is necessary to understand the potential negative effects of such intervention.

With respect to mathematical modeling of deterministic systems, a physical model of the production process was constructed using a one-dimensional diffusion equation in 2012 [1]. However, many concerns that occur in the supply chain are major problems facing production efficiency and business profitability. A stochastic partial bilinear differential equation with time delay was derived for outlet processes. The supply chain was modeled by considering as time delay [3]. With respect to the analysis of production processes in stochastic systems based on financial engineering, we have proposed that a production throughput rate can be estimated utilizing a Kalman filter based on a stochastic differential equation [2]. We have also proposed a stochastic differential equation (SDE) for the mathematical model describing production processes from the input of materials to the end. We utilized a risk-neutral principal in stochastic calculus based on the SDE [4].

With respect to the analysis of production processes based on physics, we have clarified that phenomena such as power-law distributions, self-similarity, phase transitions, and

on−off intermittency can occur in production processes [5, 6, 7, 8, 9]. On the other hand, there is the famous theory of constraints (TOC) that describes the importance of avoiding bottlenecks in production processes [10]. Small fluctuations in an upstream subsystem appear as large fluctuations in the downstream (the so-called bullwhip effect) [13]. The bullwhip effect generates a large gap between the demand forecasts of the market and suppliers. Large fluctuations can be suppressed by the following mechanisms.

(1) Reducing the lead time, improving the throughput, and synchronizing the production process by the TOC.
(2) Sharing the demand information and performing mathematical evaluations.
(3) Analyzing the reduction and fluctuating demands of the subsystem (using nonlinear vibration theory).
(4) Basing the inventory management approach on stochastic demand.

When using manufacturing equipment, delays in one production step are propagated to the next. Hence, the use of manufacturing equipment itself may lead to delays. The improvement of production processes was presented that the "Synchronization with pre-process" method was the most desirable in practice using the actual data in production flow process based on the cash flow model by using the SDE of log-normal type [11]. In essence, we have proposed the best way, which is a synchronous method using the Vasicek model for mathematical finance [12]. Then, the supply chain theme, which was a time delay in the production processes, was proposed for the throughput improvement based on a stochastic differential equation of log-normal type [13].

In this study, we investigate the use of a Riemannian manifold for modeling a production system. We observe that a production process denotes a diffusion process in a manner similar to that of the physical phenomenon. Based on the theory of constraints (TOC), one method for optimizing a production system is to synchronize the bottlenecks in the system. These bottlenecks may result from worker volatility or delivery delays caused by other companies. Synchronizing the bottlenecks tends to improve the process throughput. The TOC generally requests the improvement cycle toward the throughput (or lead time); this shortens the bottleneck. However, the TOC does not consider standard physical constraints, which serve as quantitative guidelines for production systems. In this study, we develop a throughput model for a production flow system using a Riemannian manifold, which is easier to implement than stochastic modeling methods. This model is derived from a stochastic throughput model for producing the propagation necessary to measure synchronization. We also introduce a Fisher information matrix to specify volatility. To validate the new method and clarify the synchronization processes, we perform a dynamic simulation of a production system. We also present the real synchronous and asynchronous data obtained from the production flow process.

2. **Production Systems in the Manufacturing Equipment Industry.** The production methods used in manufacturing equipment are briefly covered in this paper. More information is provided in our report. More information is provided in our report [5]. This system is considered to be a "Make-to-order system with version control", which enables manufacturing after orders are received from clients, resulting in "volatility" according to its delivery date and lead time. In addition, there is volatility in the lead time, depending on the content of the make-to-order products (production equipment).

A manufacturing process that is termed as a production flow process is shown in Figure 2. The production flow process, which manufactures low volumes of a wide variety of products, are produced through several stages in the production process. In Figure 2, the processes consist of six stages. In each step S1-S6 of the manufacturing process, materials are being produced.

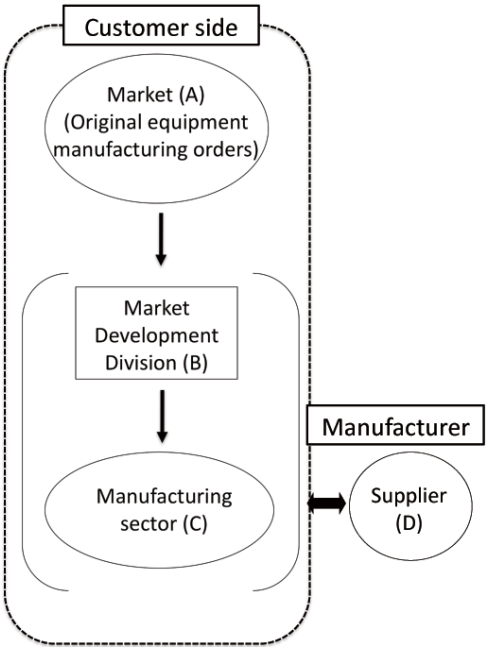

FIGURE 1. Business structure of company of research target

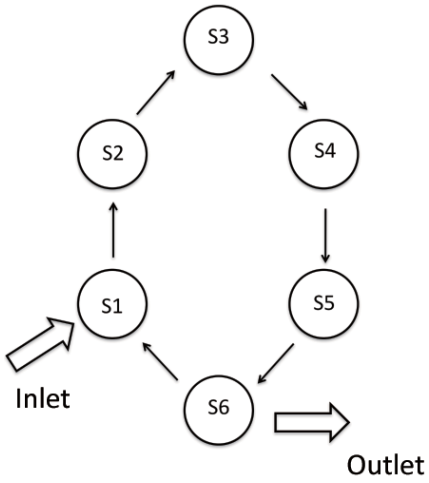

FIGURE 2. Production flow process

The direction of the arrows represents the direction of the production flow. Production materials are supplied through the inlet and the end-product is shipped from the outlet [11].

3. Mathematical Model of a Production Flow System Using a Riemannian Manifold.

3.1. Equation of harmonic mapping.

The equation of the harmonic mapping, which is an important theme of differential geometry, is decscribed as follows.

Definition 3.1. *M is a Riemannian manifold. As the harmonic map f is a stationary point, the energy functional $E(f)$ is derived as follows:*

$$E(f) = \int \frac{1}{2}|df|^2 dv_g \tag{1}$$

For a local coordinate system of M to $(x_1, x_2, \cdots, x_m)$ and $(y_1, y_2, \cdots, y_n)$, the Riemannian manifold is defined as follows:

$$g = \sum_{i,j=1}^{m} g_{ij} dx_i dx_j, \quad h = \sum_{i,j=1}^{n} h_{ij} dx_i dx_j \tag{2}$$

If an inverse matrix is written as (g_{ij}) and (h_{ij}) to (g^{ij}) and (h^{ij}), respectively, then with respect to the matrix $(y_1, y_2, \cdots, y_n)$, a Christoffel symbol to ${}^N\Gamma_{ij}^k$ is written as [24]

$${}^N\Gamma_{ij}^k = \frac{1}{2} \sum_{l=1}^{n} h^{kl} \left\{ \frac{\partial h_{jl}}{\partial y_i} + \frac{\partial h_{il}}{\partial y_j} - \frac{\partial h_{ij}}{\partial y_l} \right\} \tag{3}$$

In the same manner of Equation (3), we establish ${}^M\Gamma_{ij}^k$ with respect to $(x_1, x_2, \cdots, x_m)$ of g.

We establish Laplace operator's Δ_g of (M, g) to

$$\Delta_g = \sum_{i,j=1}^{m} g^{ij} \left\{ \frac{\partial^2}{\partial x_i \partial x_j} - \sum_{k=1}^{m} {}^M\Gamma_{ij}^k \frac{\partial}{\partial x_k} \right\} \tag{4}$$

Here, the mapping f using a local coordinate system,

$$f = (f_1, f_2, \cdots, f_n), \ f_i = y_i \circ f \tag{5}$$

$$f_i = f_i(f_1, f_2, \cdots, f_n) \tag{6}$$

From Equations (5) and (6), the equation of harmonic maps is

$$\Delta_g f^k + \sum_{i,j,k,l=1}^{m} g^{klN} \Gamma_{ij}^k(f) \frac{\partial f^i}{\partial x_k} \frac{\partial f^j}{\partial x_l} = 0, \quad k = 1, 2, \cdots, n \tag{7}$$

Equation (7) is a quasi-linear second-order elliptic type.

3.2. **Diffusion equation for production processes.** Figure 3 shows the direction of production flow from i through h. Each of the items i, j, and h has different manifolds, and each production pathway also has a different manifold. Figure 4 shows the propagation path in the Riemannian space, i.e., this figure represents the connection of the unit production process. The Riemannian manifold is equal to the sum of the differentiable manifold and distance.

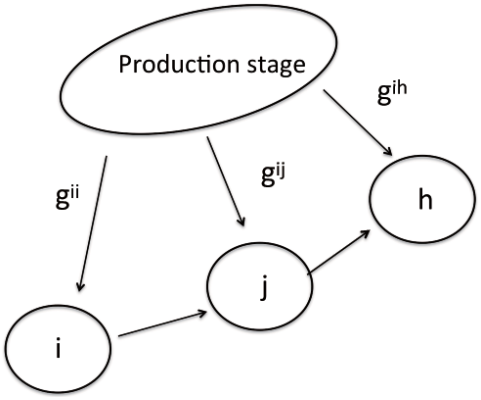

FIGURE 3. Generalized propagation connected in Riemannian space

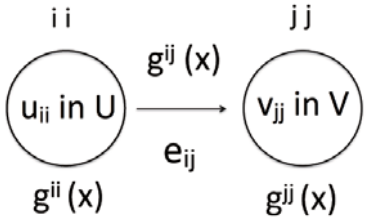

FIGURE 4. Unit propagation path in Riemannian space

Definition 3.2. *Laplace-Beltrami operator*

$$\mathcal{L}f(x) = -\sum_{i,j} g^{ij}(x) \left(\frac{\partial^2 f(x)}{\partial x^i \partial x^j} - \sum_{ik} \Gamma_{ij}^k \frac{\partial f(x)}{\partial x^k} \right) \tag{8}$$

where $[g^{ij}]$ *denotes an inverse matrix of the Riemannian metric* $[g_{ij}]$*, which is the inner product of each tangent space of the differentiable manifold.*

We now introduce a dual system of production stages. Figure 4 shows a unit propagation path in the Riemannian space.

$$Af = -div(grad_G f) + \sum_i b^i \partial_i f \tag{9}$$

where b^i is an element of the flow velocity vector and indicates that $\mathbf{b} = (\mathbf{b^1}, \mathbf{b^2}, \cdots, \mathbf{b^n})$.

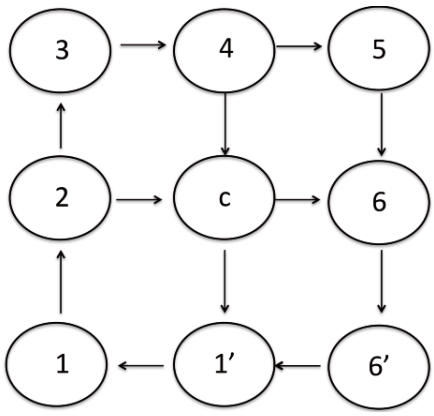

FIGURE 5. Business structure of company of research target

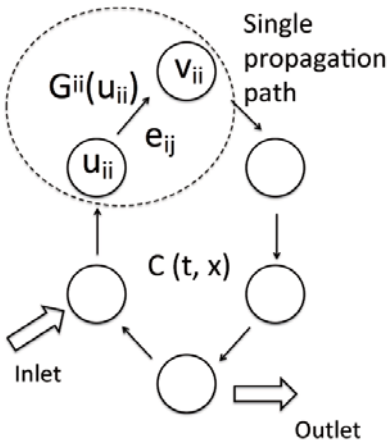

FIGURE 6. Single propagation path of $u \to v$

If an external force (control force) does not work, each process element will converge to a uniform solution; thus, the finished product will not have a set deadline. In other words, this indicates a product with a natural timeline of production.

$$\frac{\partial S(x,t)}{\partial t} = \mathcal{L}S = div(grad_G S) \tag{10}$$

The left term in Equation (10) saves the total load $\sum_{(x,t)\in\Omega\times D} S(x,t)$. Thus, the corresponding load-balancing solution is given as follows:

$$\bar{S} = \frac{\sum S(x,t)}{[\Omega \times D]} \tag{11}$$

Monotonically decrease the square error $\sum S(x,t) - \bar{S}$.

The saving of total load is as follows:

$$\int_M div(grad_G S(x,t))dx = -\int_M \mathcal{L}S(x,t)dx = 0 \tag{12}$$

$$\sum_{u\in V} \frac{\partial S(x,t)}{\partial t} = -\sum_{u\in V} \mathcal{L}S(x,t) = 0 \tag{13}$$

$\mathcal{L}S(x,t)$ has different metrics (average and volatility) that also refer to the Riemannian metric on each process and transport function:

$$\frac{d\sum_{u\in U}\left(\frac{cost}{|U|} - S\right)^2}{dt} = 2\sum_{u\in U}\left(\frac{cost}{|U|} - S\right) \times [\mathcal{S}] \tag{14}$$

where $|U|$ denotes the size of the vertex (production stage) and $cost \equiv \sum_{u\in U}(u,0)$ denotes the total load of the system.

$$\mathcal{L}S(x,t) = \sum_{i,j} g^{ij}(x)\left\{\frac{\partial^2 S(x,t)}{\partial x^i \partial x^j} - \sum_{ik} \partial_i g^{ii}(x)\right\} \tag{15}$$

Equations (15) and (16) denote the situation of Figure 4.

$$div(X) = \sum_i \partial_i X^i, \;\; grad_G f = \sum_{ij} g^{ij}\partial_j f \partial_i \tag{16}$$

Generally, Equation (17) denotes a production flow in $S(u,t)$.

$$\frac{\partial S(u,t)}{\partial t} = \mathcal{L}S(u,t) = -\sum_{ij} g^{ij}(x)\left[\frac{\partial^2 S(u,t)}{\partial x^i \partial x^j} - \sum_{ij}\partial_i g^{ii}(x)\frac{\partial S(u,t)}{\partial u}\right] \tag{17}$$

3.3. **Throughput model for a generalized production system.** We presented the stochastic throughput model in our previous study as [11]:

$$\begin{aligned}\partial C(c,t) = &\left[a(x)\frac{\partial C(x,t)}{\partial x} + D(x)\frac{\partial^2 C(x,t)}{\partial x^2}\right]\partial t \\ &+ \sum_{i=1}^{N}\partial_d^i(x)C(x,t)\partial W_d^i(x,t) + \sum_{k=1}^{N}\sigma_0^k(x)\partial W_0^k(x,t)\end{aligned} \tag{18}$$

Then, Equation (18) can be rewritten as follows:

$$\partial C(x,t) = \mathcal{L}C(x,t)dt + \sum_{i=1}^{N}\partial_d^i(x)C(x,t)\partial W_d^i(x,t) + \sum_{k=1}^{N}\sigma_0^k(x)\partial W_0^k(x,t) \tag{19}$$

where

$$\mathcal{L} \equiv \frac{1}{2}\sum_{i,j=1}^{N}\alpha^{ij}(x,t)\frac{\partial^2}{\partial x^i \partial x^j} + \sum_{i=1}^{N}\beta^i(x,t)\frac{\partial}{\partial x^i} \tag{20}$$

Equation (20) indicates an infinitesimal generator under the measure with no risk. When $\alpha^{ij}(x,t)$ and $\beta^i(x,t)$ are derived as spatial elements, Equaiton (20) can be utilized as the stochastic throughput model [4, 12]. Then, we rewrite Equaiton (20).

$$\mathcal{L} \equiv -\sum_{i,j} g^{ij}(x)\frac{\partial^2}{\partial x^i \partial x^j} - \sum_{ik}\partial_i g^{ii}(x)\frac{\partial}{\partial x^k} \tag{21}$$

where $[g^{ij}]$ indicates a reverse matrix of Riemannian metrics $[g_{ij}]$.

Definition 3.3. *Connection matrix* Γ_{ijk}

$$\Gamma_{ij}^k = \sum_h g^{hk}\Gamma_{ijh} \tag{22}$$

Then we obtain as follows [24]:

$$\partial_i g_{ih} = \Gamma_{ijh}, \quad \partial_i \equiv \frac{\partial}{\partial x^i} \tag{23}$$

Therefore, we rewrite as follows:

$$\mathcal{L} \equiv -\sum_{i,j} g^{ij}\left(\frac{\partial^2}{\partial x^i \partial x^j} - \sum_k \hat{\Gamma}_{ij}^k\frac{\partial}{\partial x^k}\right) \tag{24}$$

where

$$\partial_i g^{ik} = -\sum_{j,h} g^{hk}g^{ij}\left(\hat{\Gamma}_{ijh} + \hat{\Gamma}_{ihj}\right) \tag{25}$$

where $\hat{\Gamma}_{ijh}$ indicates the Levi-Civita connection matrix [24].

Therefore, we obtain

$$-div_G(grad_G C) = -\sum_{ij} g^{ij}\left(\frac{\partial^2}{\partial x^i \partial x^j} - \sum_k \hat{\Gamma}_{ij}^k\frac{\partial}{\partial x^k}\right) \tag{26}$$

Let the metrics of each process, including the throughput, lead time, production density, and weight, be equal to $w(u, v)$.

We represent the production model be as follows [1]:

$$\frac{\partial S(u,t)}{\partial t} = -\mathcal{L}C = div(grad_G C) \tag{27}$$

Equation (27) is represented as a diffusion equation.

Then, let the operator of stochastic model as follows:

$$\mathcal{L} \equiv div(grad_G C) \tag{28}$$

Here, we represent the mathematical model on $x \in R_+$ and $t \in R_+$ as follows:

$$\frac{\partial C(x,t)}{\partial t} = D\frac{\partial^2 C(x,t)}{\partial x^2} - v\frac{\partial C(x,t)}{\partial x} + \sigma_d C(x,t)B_d(x,t) + \sigma_0 B_0(x,t) \tag{29}$$

where, when we put $W_d(x,t)$ and $W_0(x,t)$ to Wiener process, we obtain

$$\frac{\partial W_d(x,t)}{\partial t} = B_d(x,t), \quad \frac{\partial W_0(x,t)}{\partial t} = B_0(x,t) \tag{30}$$

Therefore, from the above analysis, Equation (19) becomes:

$$\partial C(x,t) = \left[D\frac{\partial^2 C(x,t)}{\partial x^2} - v\frac{\partial C(x,t)}{\partial x}\right]\partial t + \sigma_d C(x,t)B_d(x,t) + \sigma_0 B_0(x,t) \tag{31}$$

Further, we employ an eigenvalue and eigenfunction using Green's theorem and Equation (31) then becomes:

$$dC(t) = \mu_i(t)C_i(t)dt + \sigma_d C_i(t)dW_d^i(t) + \sigma_0 dW_0^i(t), \quad i = 1, 2, \cdots \tag{32}$$

where Equation (31) has not duplication eigenvalues.

Moreover, we omit the subscript i for simplicity.

$$dC(t) = \mu(t)C(t)dt + \sigma_d C(t)dW_d(t) + \sigma_0 dW_0(t), \quad i = 1, 2, \cdots \tag{33}$$

where the mathematical model is denoted as a stationary system with external force.

$$\frac{dC(t)}{dt} = A(t)C(t) + B(t)f(t) \tag{34}$$

3.4. **Evaluation of production flow system using Fisher matrix.** We evaluate in 6 processes and 9 workers configured as shown in Figure 7.

$$\Delta g^{ii}u_{ii} \equiv g^{ii}v_{jj} - g^{ii}u_{ii} \tag{35}$$

Equation (35) denotes a discrete representation of $\partial_i g^{ii}(x)$ of the second term in Equation (21).

$$\begin{aligned}
\mathcal{L}f(u_{ii}) &= -\sum_{v_{jj}\sim u_{ii}} g^{ii}\{f(v_{jj}) - f(u_{ii})\} - \sum_{e_{ij}} \Delta g^{ii}(u_{ii})\frac{f(v_{jj}) - f(u_{ii})}{2} \\
&= -\sum_{v_{jj}\sim u_{ii}} \frac{f(v_{jj}) - f(u_{ii})}{2}\{f(v_{jj}) - f(u_{ii})\} \\
&= -\sum_{v_{jj}\sim u_{ii}} W_{ij}(u_{ii}, v_{jj})\{f(v_{jj}) - f(u_{ii})\}
\end{aligned} \tag{36}$$

Here, $W_{ij}(u_{ii}, v_{jj})$ represents propagation efficiency and is expressed as follows:

$$W_{ij}(u_{ii}, v_{jj}) = \frac{f(v_{jj}) - f(u_{ii})}{2} \tag{37}$$

where $W_{ij}(v_{jj}, u_{ii}) = W_{ij}(u_{ii}, v_{jj}) > 0$.

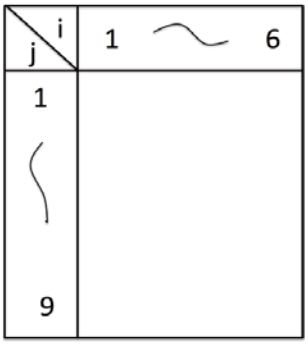

FIGURE 7. Six processes and 9 workers in production flow system

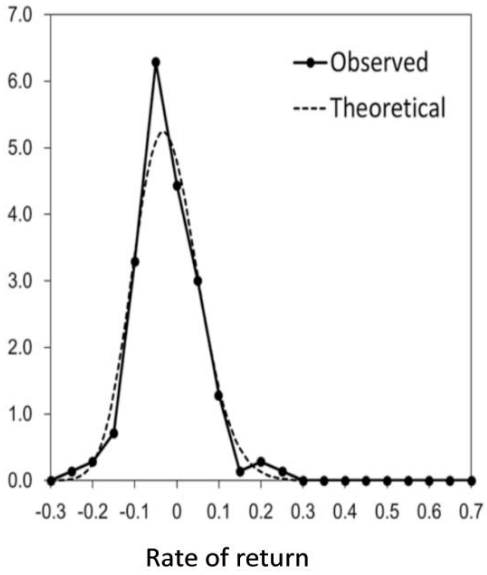

FIGURE 8. Probability density function of rate-of-return deviation: actual data (solid line) and data based on theoretical formula (dotted line)

Figure 6 shows a single propagation path of u to v, where $C(t,x)$ represents the propagation characteristics of u to v and is derived as follows:

$$\frac{\partial C(x,t)}{\partial t} = (div\ grad_G\, C) \tag{38}$$

Therefore, we obtain as follows:

$$\frac{\partial C(u,t)}{\partial t} + v\frac{\partial C(u,t)}{\partial u} = D\frac{\partial^2 C(u,t)}{\partial u^2} \tag{39}$$

Equation (39) represents a propagation equation with respect to $u, t \in V$, and $w(u,v)$ is the weight parameter of the propagation path between each stage in the process. Therefore, the square distance to the deviation of (μ_i, σ_i) in each propagation path is derived as follows:

$$ds_i^2 = \sum g_{ii}(\xi) d\xi_i d\xi_j \tag{40}$$

where $\xi_i = (\mu_i, \sigma_i)$.

Thus, let $\xi \in (\mu, \sigma)$, ds_i^2 is derived as follows:

$$ds_i^2 = (d\mu, d\sigma) G(\xi) \begin{bmatrix} d\mu \\ d\sigma \end{bmatrix} = \frac{d\mu^2 + 2d\sigma^2}{\sigma^2} \tag{41}$$

where $G(\xi)$ is Fisher matrix and is derived as follows:

$$G(\xi) = \frac{1}{\sigma^2} \begin{bmatrix} 1 & 0 \\ 0 & 2 \end{bmatrix} \tag{42}$$

According to Equation (41), it is the best way to suppress the volatility σ. This result is in agreement with previous results [11, 12, 13].

4. Verification of the Riemannian Manifold Theory.

4.1. **Log-normal distribution characteristics of rate of return.** For a small-to-midsize firm, it is of the upmost importance not to cause default in a cash flow, and it is necessary for business continuity. As is the case with rate-of-return deviation, we also analyzed a return acquisition rate defined by Equation (43). The result is shown in Figure 8 [5].

From the data of monthly rate of return observed, its probability density function was calculated (Figure 8). As a result, it was found that the probability density function conforms to log-normal distribution (Figure 8, Theoretical).

Theoretical curve was calculated using EasyFit software (http://www.mathwave.com/), and as a result of Kolmogorov and Smirnov test, the observed values conformed to a log-normal type probability density function. Because, in the goodness-of-fit test of Kolmogorov-Smirnov, a null hypothesis that it is "log-normal" was not rejected with rejection rate 0.2, and this data conforms to "log-normal" distribution. P-value was 0.588. The parameters of a theoretical curve were: $\mu_p = -0.134$ (average), $\sigma_p = 0.0873$ (standard deviation), $\gamma_p = -0.900$. The theoretical curve is given by the following formula.

$$f(x) = \frac{1}{\sqrt{2\pi}\,(x-\gamma_p)\,\sigma_p} \exp\left\{-\frac{1}{2}\left(\frac{(\ln x - \gamma_p) - \mu}{\sigma_p}\right)^2\right\} \tag{43}$$

4.2. **Dynamic simulation of production flow processes.** We performed a dynamic simulation of a production flow process using the simulation system developed by NTT DATA Mathematical Systems Inc. (www.msi.co.jp). The observed data of the monthly rate of return formed a log-normal probability distribution. The purpose of our simulation was to determine how dispersion affects the throughput. Based on the Fisher matrix of the information geometry described above, Equation (41) indicates that volatility affects

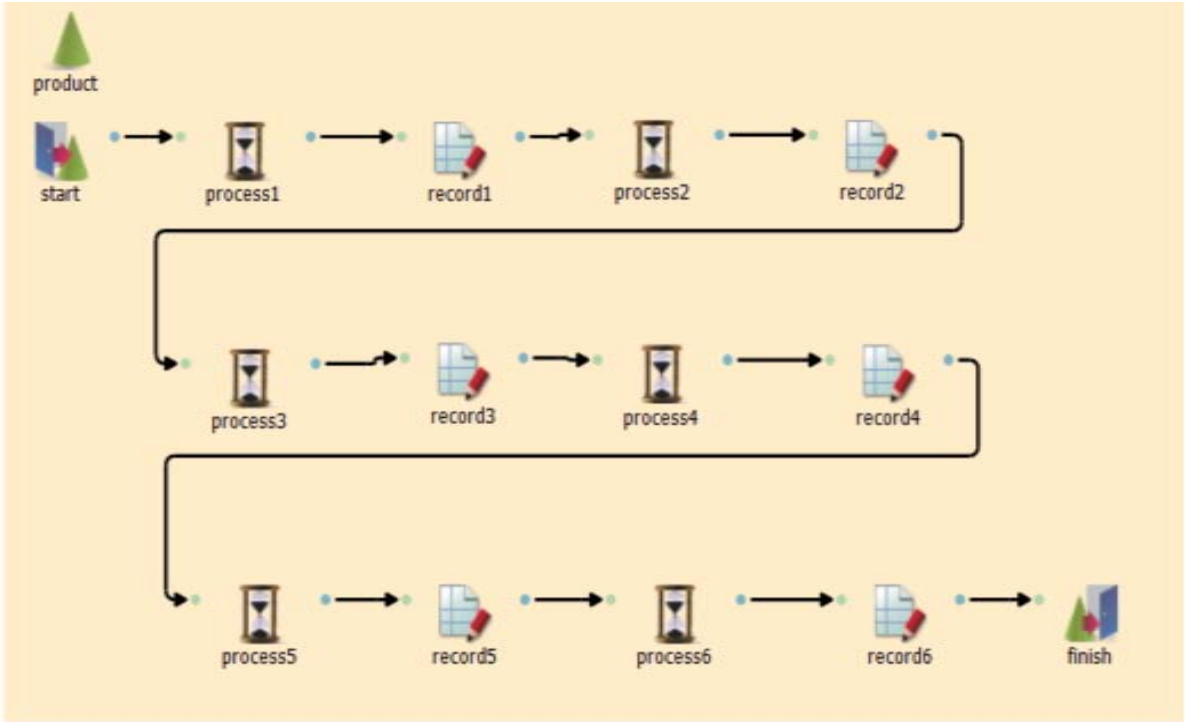

FIGURE 9. Simulation model of production flow system

the larger throughput. The simulated production flow process comprised six processes and nine workers.

With respect to the meaning of the individual parts in Figure 9, we conducted a simulation of the following procedure.

- When the simulation began, it generated one of the products on a "generate" parts going to "finish".
- In each process, including the six workers in parallel, the slowest worker waited till the work was completed.
- When the work of each process was completed, it moved to the next process.
- Simultaneously as each process was completed, it recorded the working time of each process.

With respect to Table 1 and Table 2,

- Process No. indicates each process (1-6).
- Average indicates the average time.
- STD indicates the standard deviation of process time (sec).
- Worker efficiency (WE) indicates the efficiency of six workers.

"record" calculates the worker's operating time, which is obtained by multiplying the specified WE data for the log-normally distributed random numbers in Table 1.

TABLE 1. Working data for six production asynchronous processes

Process No.	No.1	No.2	No.3	No.4	No.5	No.6
Average	20	22	25	22	25	21
STD	2.1	2.5	1.6	1.9	2.0	1.9
W.E 1	0.83	1.0	0.66	0.76	0.88	0.91
W.E 2	1.27	1.26	1.21	1.31	1.17	1.20
W.E 3	0.96	1.11	1.01	1.12	0.88	0.89
W.E 4	0.92	0.96	1.06	0.98	0.91	0.9
W.E 5	1.2	1.03	1.07	0.89	1.03	1.1
W.E 6	1.09	1.1	1.2	0.98	1.13	0.89

TABLE 2. Working data for six production synchronous processes

Process No.	No.1	No.2	No.3	No.4	No.5	No.6
Average	20	20	20	20	20	20
STD	1.1	1.5	1.2	1.4	1.0	1.4
W.E 1	1.0	1.0	1.0	1.0	1.0	1.0
W.E 2	1.0	1.0	1.2	1.3	1.1	1.2
W.E 3	1.7	1.1	1.0	1.1	1.0	1.0
W.E 4	1.0	1.0	1.0	1.0	1.0	1.0
W.E 5	1.0	1.0	1.0	1.0	1.0	1.0
W.E 6	1.0	1.3	1.2	1.0	1.1	1.0

Figure 10 shows the operating time of process 1-6 (record1-record6). As the working time of the synchronous process is less volatile, the work efficiency became higher than the asynchronous process. In Figure 10, the total working time of asynchronous and synchronous processes are 1241.7 (sec) and 586.4 (sec) respectively. The synchronous process shows much better production efficiency than the asynchronous process.

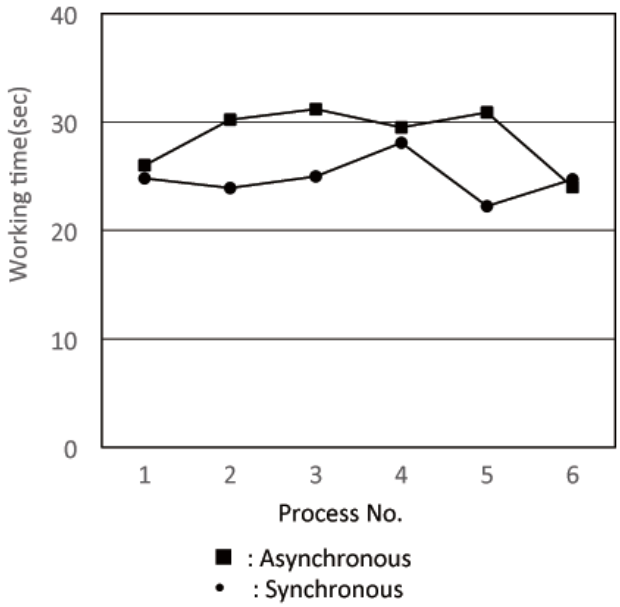

FIGURE 10. Working time for process number one through six

4.3. **Actual data example of production flow process.** The production throughput is evaluated using the number of equipment pieces in comparison with the target number of equipment pieces (production ranking) and simulating asynchronous and synchronous production (see Appendix A). The asynchronous method is prone to worker fluctuations imposed by various delays, whereas worker fluctuations in the synchronous method are small. In terms of the production lead time results presented in the Appendix, the productivity ranking tests indicate that test run 3 > test run 2 > test run 1, where test run 1 is asynchronous and test runs 2 and 3 are synchronous.

Here, the throughput values calculated from the throughput probability in test run 1-test run 3, are as follows.

- Test run 1: 4.4 (pieces of equipment)/6 (pieces of equipment) = 0.73
- Test run 2: 5.5 (pieces of equipment)/6 (pieces of equipment) = 0.92
- Test run 3: 5.7 (pieces of equipment)/6 (pieces of equipment) = 0.95

5. **Conclusion.** By using a Riemannian manifold with a Fisher information matrix, we verified that the bottlenecks in a production flow process result from worker volatilities and delivery delays caused by other companies. The results of this work allow us to obtain the quantitative constraints that are not given by the TOC. Therefore, we were able to define a stochastic throughput model for producing the propagation necessary to measure the synchronization derived by Equations (18) and (29). In addition, as a one-dimensional model, Equation (33) was defined by using Equation (30). Moreover, stationary systems can be defined by Equation (34).

Acknowledgment. We thank Dr. E. Chikayama, Associate professor of Niigata University of International and Information Studies, for verifying the log-normal distribution type data.

REFERENCES

[1] K. Shirai and Y. Amano, Prduction density diffusion equation and production, *IEEJ Trans. Electronics, Information and Systems*, vol.132-C, no.6, pp.983-990, 2012.

[2] K. Shirai and Y. Amano, A study on mathematical analysis of manufacturing lead time – Application for deadline scheduling in manufacturing system –, *IEEJ Trans. Electronics, Information and Systems*, vol.132-C, no.12, pp.1973-1981, 2012.
[3] K. Shirai and Y. Amano, Model of production system with time delay using stochastic bilinear equation, *Asian Journal of Management Science and Applications*, vol.1, no.1, pp.83-103, 2015.
[4] K. Shirai, Y. Amano and S. Omatu, Process throughput analysis for manufacturing process under incomplete information based on physical approach, *International Journal of Innovative Computing, Information and Control*, vol.9, no.11, pp.4431-4445, 2013.
[5] K. Shirai, Y. Amano, S. Omatu and E. Chikayama, Power-law distribution of rate-of-return deviation and evaluation of cash flow in a control equipment manufacturing company, *International Journal of Innovative Computing, Information and Control*, vol.9, no.3, pp.1095-1112, 2013.
[6] K. Shirai and Y. Amano, Self-similarity of fluctuations for throughput deviations within a production process, *International Journal of Innovative Computing, Information and Control*, vol.10, no.3, pp.1001-1016, 2014.
[7] K. Shirai, Y. Amano and S. Omatu, Consideration of phase transition mechanisms during production in manufacturing processes, *International Journal of Innovative Computing, Information and Control*, vol.9, no.9, pp.3611-3626, 2013.
[8] K. Shirai and Y. Amano, Calculating phase transition widths in production flow processes using an average regression model, *International Journal of Innovative Computing, Information and Control*, vol.11, no.3, pp.1075-1091, 2015.
[9] K. Shirai and Y. Amano, On-off intermittency management for production process improvement, *International Journal of Innovative Computing, Information and Control*, vol.11, no.3, pp.815-831, 2015.
[10] S. J. Baderstone and V. J. Mabin, A review goldratt's theory of constraints (TOC) – Lessons from the international literature, *Operations Research Society of New Zealand the 33rd Annual Conference*, University of Auckland, New Zealand, 1998.
[11] K. Shirai, Y. Amano and S. Omatu, Improving throughput by considering the production process, *International Journal of Innovative Computing, Information and Control*, vol.9, no.12, pp.4917-4930, 2013.
[12] K. Shirai and Y. Amano, Production throughput evaluation using the Vasicek model, *International Journal of Innovative Computing, Information and Control*, vol.11, no.1, pp.1-17, 2015.
[13] K. Shirai, Y. Amano and S. Omatu, Propagation of working-time delay in production, *International Journal of Innovative Computing, Information and Control*, vol.10, no.1, pp.169-182, 2014.
[14] K. Shirai and Y. Amano, Application of an autonomous distributed system to the production process, *International Journal of Innovative Computing, Information and Control*, vol.10, no.4, pp.1247-1265, 2014.
[15] K. Shirai and Y. Amano, Throughput improvement strategy for nonlinear characteristics in the production processes, *International Journal of Innovative Computing, Information and Control*, vol.10, no.6, pp.1983-1997, 2014.
[16] K. Shirai and Y. Amano, Validity of production flow determined by the phase difference in the gradient system of an autonomous decentralized system, *International Journal of Innovative Computing, Information and Control*, vol.10, no.5, pp.1727-1745, 2014.
[17] K. Shirai and Y. Amano, Analysis of production processes using a lead-time function, *International Journal of Innovative Computing, Information and Control*, vol.12, no.1, pp.125-138, 2016.
[18] R. Benzi, A. Sutera and A. Vulpiani, The mechanism of stochastic resonance, *Journal of Physics A: Mathematical and General*, vol.14, no.11, pp.453-457, 1981.
[19] S. Ishiwata and K. Koizumi, Weak signal detection and its applications by stochastic resonance, *Phenomena and Mathematical Theory of Nonlinear Waves and Nonlinear Dynamical Systems*, Reports of RIAM Symposium No.17ME-S2, 2005.
[20] H. Fujisaka, T. Kamio and K. Ikuiwa, Stochastic resonance in coupled sychronization loops, *IEICE*, vol.J90-A, no.11, pp.806-816, 2007.
[21] A. A. Stanislavsky, Fractional dynamics from the ordinary Langevin equation, *Physical Review*, vol.E67, pp.021111-1-021111-6, 2003.
[22] M. Sugi, H. Yuasa and T. Arai, Autonomous decentralized control of traffic signal network by reaction-diffusion equations on a graph, *Journal of SICE*, vol.39, no.1, pp.51-58, 2003.
[23] K. Kitahara, *Nonequilibrium Statistical Mechanics*, Iwanami Co., LTD, 2000.
[24] Y. Matsumoto, *Foundation of the Manifold (Basic Math5)*, University of Tokyo Press, 1988.

Appendix A. **Analysis of Actual Data in the Production Flow System.** Figure 2 represents a manufacturing process called a flow production system, which is a manufacturing method employed in the production of control equipment. The flow production system, which in this case has six stages, is commercialized by the production of material in steps S1-S6 of the manufacturing process.

The direction of the arrow represents the direction of the production flow. In this system, production materials are supplied from the inlet and the end product will be shipped from the outlet.

Assumption A.1. *The production structure is nonlinear.*

Assumption A.2. *The production structure is a closed structure; that is, the production is driven by a cyclic system (production flow system).*

Assumption A.1 indicates that the determination of the production structure is considered as a major factor, which includes the generation value of production or the throughput generation structure in a stochastic manufacturing process (hereafter called the manufacturing field). Because such a structure is at least dependent on the demand, it is considered to have a nonlinear structure.

Because the value of such a product depends on the throughput, its production structure is nonlinear. Therefore, Assumption A.1 reflects the realistic production structure and is somewhat valid. Assumption A.2 is completed in each step and flows from the next step until stage S6 is completed. Assumption A.2 is reasonable because new production starts from S1.

Based on the control equipment, the product can be manufactured in one cycle. The production throughput required to maintain 6 pieces of equipment/day is as follows:

$$\frac{(60 \times 8 - 28)}{3} \times \frac{1}{6} \simeq 25 \text{ (min)} \tag{44}$$

where the throughput of the previous process is set as 20 (min). In Equation (44), "28" represents the throughput of the previous process plus the idle time for synchronization. "8" is the number of processes and the total number of all processes is "8" plus the previous process. "60" is given by 20 (min) $\times$ 3 (cycles).

One process throughput (20min) in full synchronization is

$$T_s = 3 \times 120 + 40 = 400 \text{ (min)} \tag{45}$$

Therefore, a throughput reduction of about 10% can be achieved. However, the time between processes involves some asynchronous idle time.

As a result, the above test-run is as follows.

- (test run 1): Each throughput in every process (S1-S6) is asynchronous, and its process throughput is asynchronous. Table 3 represents the manufacturing time (min) in each process. Table 4 represents the variance in each process performed by workers. Table 3 represents the target time, and the theoretical throughput is given by $3 \times 199 + 2 \times 15 = 627$ (min).

  In addition, the total working time in stage S3 is 199 (min), which causes a bottleneck. Figure 11 is a graph illustrating the measurement data in Table 3, and it represents the total working time for each worker (K1-K9). The graph in Figure 12 represents the variance data for each working time in Table 3.
- (test run 2): Set to synchronously process the throughput.

  The target time in Table 5 is 500 (min), and the theoretical throughput (not including the synchronized idle time) is 400 (min). Table 6 represents the variance data of each working process (S1-S6) for each worker (K1-K9).

TABLE 3. Total manufacturing time at each stage for each worker

	WS	S1	S2	S3	S4	S5	S6
K1	15	(20)	(20)	(25)	(20)	(20)	(20)
K2	20	(22)	(21)	(22)	(21)	(19)	(20)
K3	10	(20)	(26)	(25)	(22)	(22)	(26)
K4	20	17	15	19	18	16	18
K5	15	15	(20)	(18)	(16)	15	15
K6	15	15	15	15	15	15	15
K7	15	(20)	(20)	(30)	(20)	(21)	(20)
K8	20	(29)	(33)	(30)	(29)	(32)	(33)
K9	15	14	14	15	14	14	14
Total	145	172	184	199	175	174	181

TABLE 4. Volatility of Table 3

K1	1.67	1.67	3.33	1.67	1.67	1.67
K2	2.33	2	2.33	2	1.33	1.67
K3	1.67	3.67	3.33	2.33	2.33	3.67
K4	0.67	0	1.33	1	0.33	1
K5	0	1.67	1	0.33	0	0
K6	0	0	0	0	0	0
K7	1.67	1.67	5	1.67	2	1.67
K8	4.67	6	5	4.67	5.67	6
K9	0.33	0.33	0	0.33	0.33	0.33

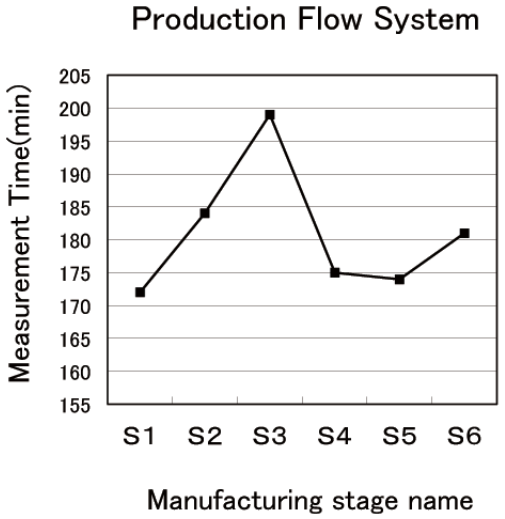

FIGURE 11. Total work time for each stage (S1-S6) in Table 3

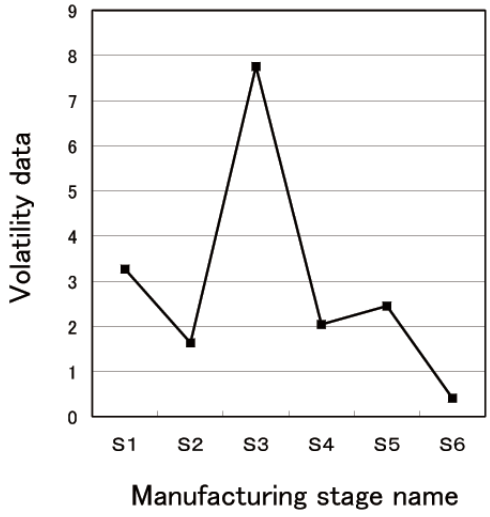

FIGURE 12. Volatility data for each stages (S1-S6) in Table 3

TABLE 5. Total manufacturing time at each stage for each worker

	WS	S1	S2	S3	S4	S5	S6
K1	20	20	(24)	20	20	20	20
K2	20	20	20	20	20	22	20
K3	20	20	20	20	20	20	20
K4	20	(25)	(25)	20	20	20	20
K5	20	20	20	20	20	20	20
K6	20	20	20	20	20	20	20
K7	20	20	20	20	20	20	20
K8	20	(27)	(27)	(22)	(23)	20	20
K9	20	20	20	20	20	20	20
Total	180	192	196	182	183	182	180

TABLE 6. Volatility of Table 5

K1	0	1.33	0	0	0	0
K2	0	0	0	0	0.67	0
K3	0	0	0	0	0	0
K4	1.67	1.67	0	0	0	0
K5	0	0	0	0	0	0
K6	0	0	0	0	0	0
K7	0	0	0	0	0	0
K8	2.33	2.33	0.67	1	0	0
K9	0	0	0	0	0	0

TABLE 7. Total manufacturing time at each stage for each worker

	WS	S1	S2	S3	S4	S5	S6
K1	20	18	19	18	20	20	20
K2	20	18	18	18	20	20	20
K3	20	21	21	21	20	20	20
K4	20	13	11	11	20	20	20
K5	20	16	16	17	20	20	20
K6	20	18	18	18	20	20	20
K7	20	14	14	13	20	20	20
K8	20	22	22	20	20	20	20
K9	20	25	25	25	20	20	20
Total	180	165	164	161	180	180	180

TABLE 8. Variance of Table 7

K1	0.67	0.33	0.67	0	0	0
K2	0.67	0.67	0.67	0	0	0
K3	0.33	0.33	0.33	0	0	0
K4	2.33	3	3	0	0	0
K5	1.33	1.33	1	0	0	0
K6	0.67	0.67	0.67	0	0	0
K7	2	2	2.33	0	0	0
K8	0.67	0.67	0	0	0	0
K9	1.67	1.67	1.67	0	0	0

- (test run 3): The process throughput is performed synchronously with the reclassification of the process. The theoretical throughput (not including the synchronized idle time) is 400 (min) in Table 7.

  Table 8 represents the variance data of Table 7. "WS" in the measurement tables represents the standard working time. This is an empirical value obtained from long-term experiments.